SAND2015-7872J

AIP | Applied Physics Letters

Bonding between graphene and MoS2 monolayers without and with Li intercalation

Towfiq Ahmed, N. A. Modine, and Jian-Xin Zhu

Citation: Applied Physics Letters **107**, 043903 (2015); doi: 10.1063/1.4927611
View online: http://dx.doi.org/10.1063/1.4927611
View Table of Contents: http://scitation.aip.org/content/aip/journal/apl/107/4?ver=pdfcov
Published by the AIP Publishing

Articles you may be interested in

Electrochromism and small-polaron hopping in oxygen deficient and lithium intercalated amorphous tungsten oxide films
J. Appl. Phys. **118**, 024901 (2015); 10.1063/1.4926488

Tunable MoS2 bandgap in MoS2-graphene heterostructures
Appl. Phys. Lett. **105**, 031603 (2014); 10.1063/1.4891430

Substrate induced modulation of electronic, magnetic and chemical properties of MoSe2 monolayer
AIP Advances **4**, 047107 (2014); 10.1063/1.4871080

Strain-induced magnetism in MoS2 monolayer with defects
J. Appl. Phys. **115**, 054305 (2014); 10.1063/1.4864015

Electronic structure and optical conductivity of two dimensional (2D) MoS2: Pseudopotential DFT versus full potential calculations
AIP Conf. Proc. **1447**, 1269 (2012); 10.1063/1.4710474

This article is copyrighted as indicated in the article. Reuse of AIP content is subject to the terms at: http://scitation.aip.org/termsconditions. Downloaded to IP: 198.102.153.1 On: Mon, 14 Sep 2015 22:11:18

Bonding between graphene and MoS_2 monolayers without and with Li intercalation

Towfiq Ahmed,[1,a)] N. A. Modine,[2] and Jian-Xin Zhu[1,3,b)]
[1]*Theoretical Division, Los Alamos National Laboratory, Los Alamos, New Mexico 87545, USA*
[2]*Center for Integrated Nanotechnologies, Sandia National Laboratories, Albuquerque, New Mexico 87185, USA*
[3]*Center for Integrated Nanotechnologies, Los Alamos National Laboratory, Los Alamos, New Mexico 87545, USA*

(Received 13 May 2015; accepted 14 July 2015; published online 29 July 2015)

We performed density functional theory (DFT) calculations for a bi-layered heterostructure combining a graphene layer with a MoS_2 layer with and without intercalated Li atoms. Our calculations demonstrate the importance of the van der Waals (vdW) interaction, which is crucial for forming stable bonding between the layers. Our DFT calculation correctly reproduces the linear dispersion, or Dirac cone, feature at the Fermi energy for the isolated graphene monolayer and the band gap for the MoS_2 monolayer. For the combined graphene/MoS_2 bi-layer, we observe interesting electronic structure and density of states (DOS) characteristics near the Fermi energy, showing both the gap like features of the MoS_2 layer and in-gap states with linear dispersion contributed mostly by the graphene layer. Our calculated total DOS in this vdW heterostructure reveals that the graphene layer significantly contributes to pinning the Fermi energy at the center of the band gap of MoS_2. We also find that intercalating Li ions in between the layers of the graphene/MoS_2 heterostructure enhances the binding energy through orbital hybridizations between cations (Li adatoms) and anions (graphene and MoS_2 monolayers). Moreover, we calculate the dielectric function of the Li intercalated graphene/MoS_2 heterostructure, the imaginary component of which can be directly compared with experimental measurements of optical conductivity in order to validate our theoretical prediction. We observe sharp features in the imaginary component of the dielectric function, which shows the presence of a Drude peak in the optical conductivity, and therefore metallicity in the lithiated graphene/MoS_2 heterostructure. © *2015 AIP Publishing LLC*.
[http://dx.doi.org/10.1063/1.4927611]

Currently, Li-ion batteries (LIB) are a very popular power source for portable electronic devices and hybrid vehicles. However, despite being renewable and environmentally friendly, conventional Li-ion batteries are still far from meeting the national U.S. ABC target for a cheap ($150/kW h) and high capacity (3000 kW h/kg) power source.[1] This is mostly due to the widespread use of graphite based anodes in LIB, which only have a small theoretical specific capacity (372 mA h/g).[2] Thus, the development of the next generation LIB calls for identifying alternative materials for the negative and positive electrodes. In this respect, both graphene and MoS_2 monolayers have demonstrated potential as materials for designing superior electrodes with high specific capacity. High capacities from 600 to 1000 mA h/g have been observed for single atomically thin graphene nanosheets.[3–6] Moreover, several experimental works[7,8] on transition metals and metal oxides supported on graphene as negative electrodes have shown enhanced performance for LIB. On the other hand, the usage of a transition metal sulfide MoS_2, with graphene like structure, was proposed as a potential anode material in a patent in 1980.[9] Despite its high insertion capacity (≈1000 mA h/g), MoS_2 alone has not been realized as the primary anode material due to its low cyclic stability.[4] Therefore, new design principles for MoS_2-based anode materials should be explored. Some recent experimental work[10] has also demonstrated the potential of graphene/MoS_2 as the anode material for LIB.

In this letter, we propose to use graphene and MoS_2 van der Waals (vdW) bilayers[11] as an anode material for Li atoms.[4] Our study is carried out within the framework of density functional theory (DFT). We start with the consideration of the bonding properties of graphene and MoS_2 bilayers without Li intercalation. Our results show orbital hybridization between the layers, where the vdW interaction dominantly contributes to the stability of the heterostructure with significant binding energy. A shift in chemical potential is also observed in our calculations for the graphene/MoS_2 bilayer when compared with the isolated graphene or MoS_2 mono layers. Particularly noticeable is the linear dispersion in the DOS near the Fermi energy of the graphene/MoS_2 bilayer, which resembles that of the isolated graphene monolayer. Thus, combining graphene with a MoS_2 layer helps to pin the chemical potential near the gap center of MoS_2 and creates semi-metal like electronic structure in the heterostructure.

Our DFT calculation shows an even larger binding energy when the graphene/MoS_2 bilayer is intercalated with Li ions. The higher stability in such heterostructure makes it a potential candidate for designing LIB anodes with larger specific capacity and longer cycle life-time. The hybridization between carbon *p*, lithium *s*, and molybdenum *d* orbitals

[a)]Electronic mail: atowfiq@lanl.gov
[b)]Electronic mail: jxzhu@lanl.gov

 © 2015 AIP Publishing LLC

This article is copyrighted as indicated in the article. Reuse of AIP content is subject to the terms at: http://scitation.aip.org/termsconditions. Downloaded to IP: 198.102.153.1 On: Mon, 14 Sep 2015 22:11:18

causes the chemical potential to shift into the *d*-bands making the Li intercalated heterostructure fully metallic. The resulting enhancement of the conductivity in lithiated graphene/MoS_2 heterostructure is highly desirable for the anode materials in LIB.

Earlier theoretical works[12] have demonstrated similar chemical potential shift using various adatoms in addition to Li, for single and bilayer graphene. For a related graphene and MoS_2 heterostructure, Miwa and Scopel[13] reported the DFT calculated density of states (DOS) without observing any Fermi energy pinning or linear dispersion near the gap center of MoS_2. Comparing the calculated binding energy of graphene and MoS_2 bilayer, we observe an approximately 40 meV difference between this work and Ref. 13. Such mismatch possibly stems from the different vdW functionals used in these calculations. In Ref. 13, revPBE-vdW functional[14] was used for the calculations. This particular functional may cause significant under-binding up to even hundred meV compared to optB86b-vdW which was demonstrated by Klimeš *et al.*[15] Furthermore, we notice difference in the DOS between this work and that of Ref. 13. Both in this work and Ref. 13, the vdW interaction is found to play a dominant role for binding graphene with MoS_2 layer. This suggests a weak electronic hybridization between the layers. But in contrast, the DOS presented in Fig. 1(c) of Ref. 13 remarkably suggest strong electronic hybridization between graphene and MoS_2 layers, which can be realized from the absence of any graphene like features in the solid black curve (for MoS_2/Li/graphene) comparing to the red curve (MoS_2/Li). According to this result, the semi-metallicity of graphene (Dirac cone at Fermi energy) is completely lost, and the combined bilayer system becomes insulating. In contrast, our calculations suggest simultaneous presence of graphene and MoS_2 electronic features near the Fermi energy in the combined system due to the weak electronic hybridization between the layers. Thus, the Fermi energy can be pinned in the combined system due to the Dirac cone feature contributed by the weakly interacting graphene layer. In this letter, we have demonstrated the interesting Dirac dispersion characteristics in the electronic DOS of graphene/MoS_2 bilayer at the Fermi energy. Although the lithiation makes the compound metallic as expected, discharging of LIB gradually turns the anode into semimetal while retaining the stability. In the language of electrochemistry, such processes can be presented by the following two half-reactions:[16] in anode

$$xLiC_6/(MoS_2)_5 \underset{discharge}{\overset{charge}{\rightleftarrows}} xLi^+ + xe^- + C_6/(MoS_2)_5,$$

and in cathode

$$Li_{1-x}CoO_2 + xLi^+ + xe^- \underset{discharge}{\overset{charge}{\rightleftarrows}} LiCoO_2.$$

Here, due to the lattice parameter mismatch, we take 6 unit cells of graphene and 5 unit cells of MoS_2 in each direction of our supercell, as shown in Fig. 1 (see below for more details).

Therefore, our proof-of-principles calculations demonstrate the Li intercalated graphene/MoS_2 bilayer as potential candidates for designing high performance anode materials for the next generation LIBs.

All calculations in this paper are performed using the plane-wave pseudo-potential code VASP[17–19] under the generalized gradient approximation of Perdew, Burke, and Ernzerhof (PBE).[20] For atomic core-levels, we have used projected augmented wave (PAW) potentials[21,22] treating the $2s2p$ of C, $2s$ of Li, $4p5s4d$ of Mo, and $3s3p$ of S as the explicit valence electrons. For all calculations, the total energy during electronic relaxation is converged to 10^{-6} eV, while the force/atom during ionic relaxation is converged to 0.01 eV/Å. A maximum energy cutoff of 500 eV is used for plane-wave basis set.

In the *xy*-plane, 6×6 unit cells of graphene and 5×5 unit cells of MoS_2 are placed in a super-cell with $a = b$

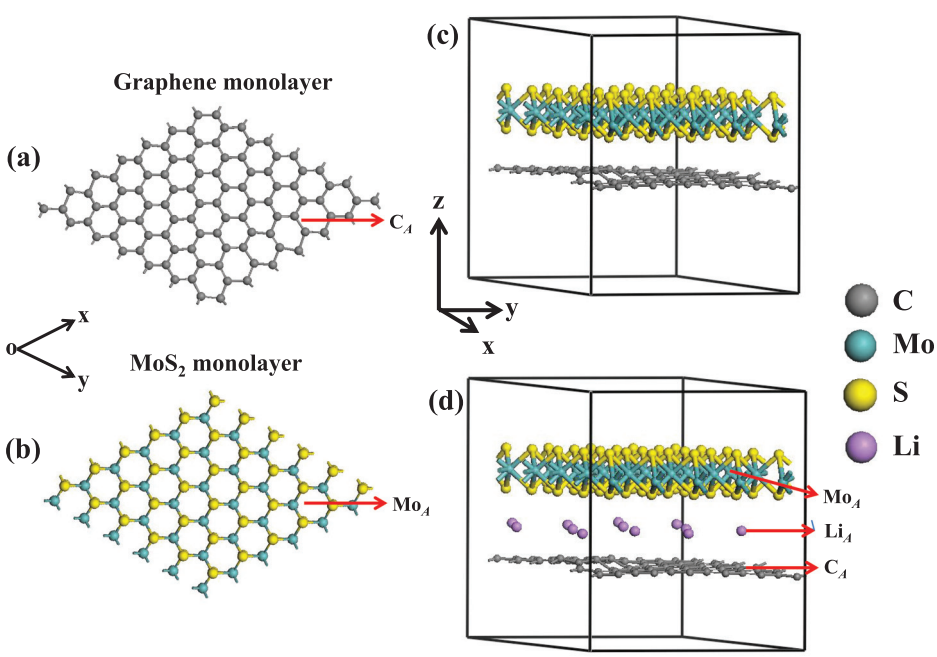

FIG. 1. Image of (a) graphene monolayer, (b) MoS_2 monolayer, (c) unit cell for graphene/MoS_2 bilayer, and (d) unit cell for Li intercalated graphene/MoS_2 bilayer. For a particular Li atom, Li_A, the nearest Mo and C atoms are denoted with Mo_A and C_A.

This article is copyrighted as indicated in the article. Reuse of AIP content is subject to the terms at: http://scitation.aip.org/termsconditions. Downloaded to IP: 198.102.153.1 On: Mon, 14 Sep 2015 22:11:18

$= 16$ Å, $c = 40$ Å, $\alpha = \beta = 90°$, and $\gamma = 120°$. In our calculations, the Li atoms are intercalated between the graphene and MoS_2 layers at the center of the graphene honeycomb sites. For different metal ions, this location has been shown to have the largest binding energies by Chan *et al.*[12] We have placed 12 Li atoms homogeneously in our super-cell. This sparse distribution of Li atoms approximates the interaction of isolated Li atoms with graphene and MoS_2. The distance between Li atoms are large enough ($\approx$7 Å) to minimize the orbital overlap between neighboring Li atoms.

To incorporate the vdW interaction between the graphene and MoS_2 layers, we have used optB86b-vdW functional where the exchange functionals were optimized for the correlation part.[23] Therefore, the local density approximation correlation part present in the PBE functional is removed by using the parameter AGGAC = 0.000 in the input file in order to avoid double-counting.

Calculations for the isolated 6×6 graphene, 5×5 MoS_2, and 6×6 graphene + Li adatoms were performed using the same sized super-cell. For ionic relaxation of graphene + Li, graphene + MoS_2, and graphene + Li + MoS_2 systems, we have used the Γ point to sample the Brillouin zone, while for all other calculations, e.g., DOS and dielectric functions, we used equally distributed 80 *k*-points in the irreducible Brillouin zone. For the calculation of dielectric function, we have used LEPSILON = .TRUE. in VASP calculation. This is the linear response or density functional perturbation (DFPT) method where the macroscopic dielectric function is calculated without and with local field effects within DFT using random phase approximation (RPA) following Gajdoš *et al.*[24]

To estimate the adsorption energy, we define

$$\Delta E = E_A + E_B - E_{A+B}, \tag{1}$$

where E_{A+B} is the total energy of the A + B composite system and E_A/E_B is the total energy of the isolated A/B constituent system.

In Table I, we present our DFT calculated total energy for graphene, MoS_2, the graphene/MoS_2 heterostructure, and the lithiated graphene/MoS_2 heterostructure. Using Eq. (1), we calculate the binding energy between graphene and MoS_2 bilayer with and without Li ions in between. We have 25 Mo atoms in our supercell, and scaled the total adsorption energy to obtain ΔE per Mo ion. We find the ΔE per Mo ion is enhanced by about three times when Li intercalation is considered. Without Li atoms, the graphene and MoS_2 layers form a physisorbed heterostructure with $\approx$0.1873 eV adsorption energy per Mo ion, where the most important contribution comes from the surface van der Waals interaction. The adsorption energy significantly increases in the presence of intercalated Li ions, and these higher adsorption energies (0.6 eV per Mo ion or 1.26 eV per Li ion) suggest a more stable structure. At the same time, the small change in atomic positions during the ionic relaxation clearly indicates the process is dominantly van der Waals driven physisorption. Thus, the Li ions are easily separable and lithiation process can be reversed. This is a highly desirable criterion for LIBs during ionization-deionization process which enhances the cycle lifetime of batteries. In the relaxed structure without Li, the average distance between C and Mo atoms is $\approx$4.5Å, where distance between C with nearest S atoms is $\approx$3.0Å. When Li is inserted in between the layers, the average distance between C and Li atoms is $\approx$2.24Å. With lithiation, the distance between C and Mo atoms is now $\approx$5.3Å.

The electronic structure of the isolated graphene and MoS_2 monolayers is changed near the Fermi energy when they are assembled to form a van der Waals heterostructure. In Fig. 2, we present the DOS for the graphene/MoS_2 bilayer systems with and without lithiation and compare with the DOS of the constituent monolayers. A graphene monolayer is a two dimensional Dirac material with linear dispersion near the Fermi energy.[25,26] This property manifests by the cone like feature in the DOS of graphene at the Fermi energy as shown in Fig. 2(a).

On the other hand, MoS_2 monolayer is a direct gap semiconductor with $\approx$1.8 eV band gap.[27] In our DFT calculations, this band gap is estimated to be 1.4 eV, as shown in Fig. 2(b). Due to the ground state nature of DFT method, the estimated band gaps are often inaccurate. Thus, in order to correctly estimate for the low lying conduction bands, one can incorporate quasi-particle self-energy corrections such as GW[28] or hybrid functionals HSE[29] approach, which accounts for the missing 0.4 eV band gap in MoS_2. In the present proof-of-principles calculations, our findings should remain unaffected from such band gap correction, while incorporating these corrections in large supercell with vdW interaction would greatly increase the computational cost. Therefore, we neglect such band-gap corrections in our calculations.

We plot the total DOS of graphene/MoS_2 in Fig. 2(c) with solid red curve. To provide visual clarity, total DOS is scaled down by a factor of 50 while comparing with the partial *d*-DOS (blue) of Mo in MoS_2 and *p*-DOS (black) of C in graphene. We find the presence of both the Dirac-cone-like feature from graphene and a gap-like feature from MoS_2 at the Fermi energy of the composite bilayer of graphene/MoS_2. An enlarged version of these symmetric features in the DOS at E_F is presented in the inset of Fig. 2(c). This finding can be interpreted as the Fermi energy pinning at the gap center of MoS_2 with the Dirac states contributed from the graphene monolayer. Such pinning of E_F cannot be identified in the isolated MoS_2 monolayer where the exact location of the chemical potential is arbitrary inside the gap. The effect of lithiation on the DOS is shown in Fig. 2(d). Using the

TABLE I. Binding energy of graphene and MoS_2 interface with and without Li intercalation using DFT + vdW.

	Graphene	MoS_2	Graphene + Li	Graphene/MoS_2	Graphene/MoS_2 + Li
Total energy (eV)	−553.25348	−414.14277	−571.97493	−972.07776	−1001.27726
Binding energy (eV)				0.1873 (per Mo ion)	0.6064 (per Mo ion) 1.2633 (per Li ion)

This article is copyrighted as indicated in the article. Reuse of AIP content is subject to the terms at: http://scitation.aip.org/termsconditions. Downloaded to IP: 198.102.153.1 On: Mon, 14 Sep 2015 22:11:18

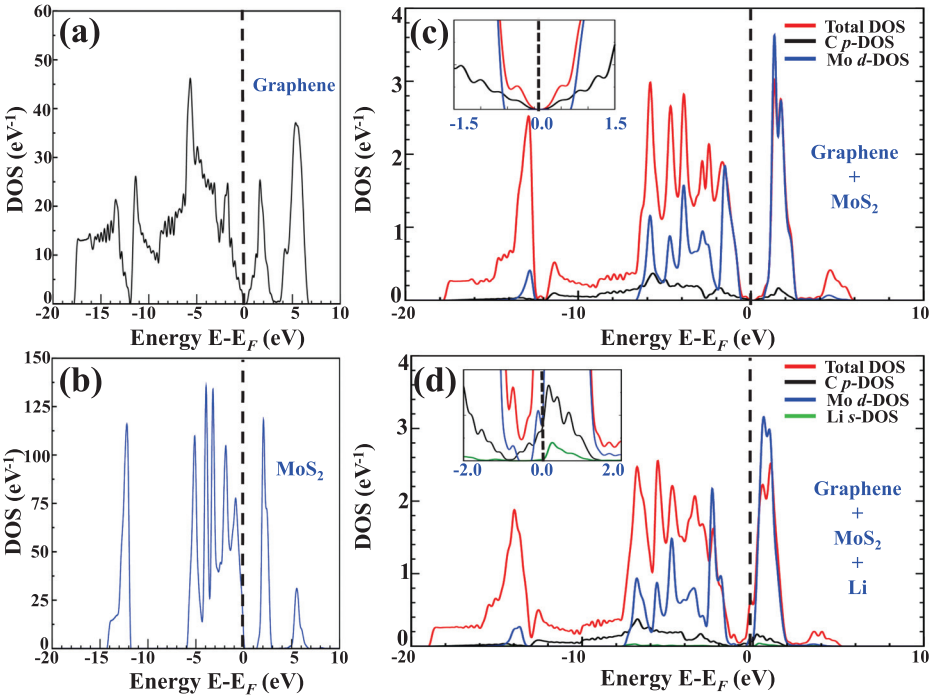

FIG. 2. (a) Total DOS (black) for graphene; (b) total DOS (blue) for MoS_2; (c) total DOS (red) for graphene/MoS_2 heterostructure, orbital projected *d*-DOS of Mo (blue), and *p*-DOS (black) for C; and (d) total DOS (red), *d*-DOS (blue) of Mo in MoS_2, *p*-DOS (black) of C in graphene, and *s*-DOS (green) of Li in the lithiated graphene/MoS_2 heterostructure; the Fermi energy is at 0 eV, shown by the vertical dashed line. Total DOS in the unit cell (for (c) and (d)) are scaled down by a factor of 50 for visual clarity. Inset in (c) and (d) shows DOS near the Fermi level.

similar scaling, we compare the total DOS with that of the partial *d*, *p*, and *s* orbitals of Mo, C, and Li atoms. The Mo and C atoms are selected from the MoS_2 and graphene layers, which are closest to a particular Li atom. These atoms are labeled in Fig. 1(d). However, we find the DOS is no longer symmetric in the presence of Li adatoms. Due to a strong hybridization between Li *s*, Mo *d*, and C *p* orbitals as well as the electron doping effect of Li, the chemical potential is shifted towards the unoccupied *d* bands, and thus, composite system becomes metallic. This implies that the loss of electrons from Li to the graphene and MoS_2 layers leads to a strong Coulomb interaction between Li ions and charged layers. It explains our observation of an increased binding energy with Lithiation. The corresponding band-structure and DOS for each case are shown in the supplementary material.[30] We note the presence of Dirac cone in the combined bilayer system which helps pinning the Fermi energy. The survival of this feature also indicates the weak electronic interaction between the layers in the absence of Li ions.

Our calculations for the real and imaginary part of dielectric function are presented in Fig. 3. Imaginary dielectric function has a direct relation to the optical conductivity via[31]

$$\mathrm{Re}\,\sigma_{\alpha\beta}(\omega) = \frac{\omega}{4\pi}\mathrm{Im}\,\epsilon_{\alpha\beta}(\omega). \tag{2}$$

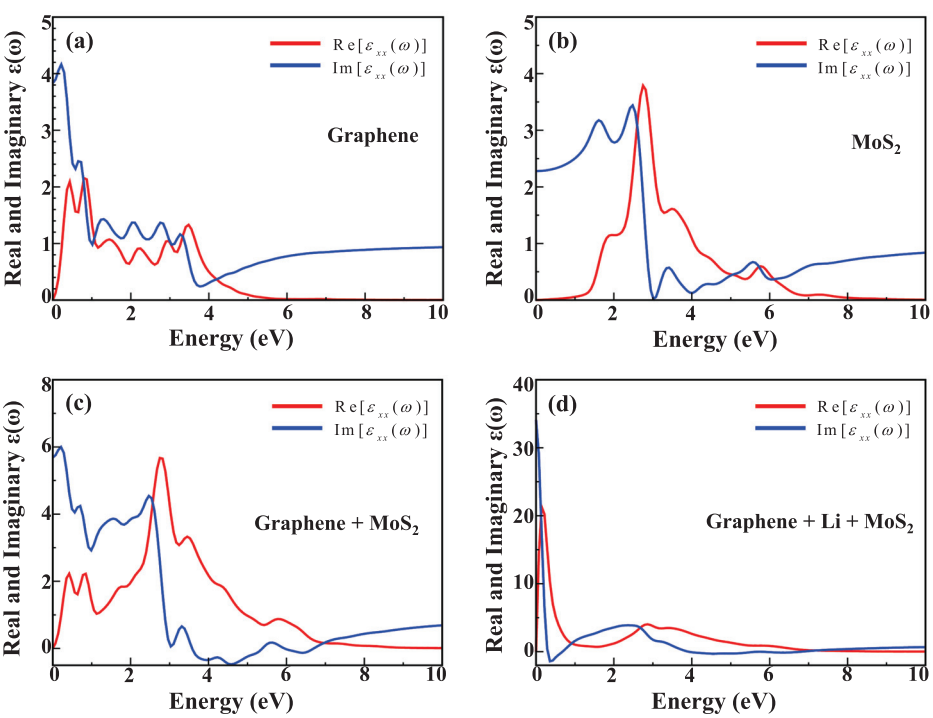

FIG. 3. Calculated real (blue) and imaginary (red) part of the dielectric function for (a) graphene, (b) MoS_2, (c) graphene/MoS_2 bilayer, and (d) Li intercalated graphene/MoS_2 heterostructure. Due to the proportionality between optical conductivity and imaginary dielectric function, such results can be directly compared with experimental measurements. See the main text for details.

This article is copyrighted as indicated in the article. Reuse of AIP content is subject to the terms at: http://scitation.aip.org/termsconditions. Downloaded to IP: 198.102.153.1 On: Mon, 14 Sep 2015 22:11:18

While the conducting nature of graphene can be understood by the sharp rise of the peak at the zero frequency as shown in Fig. 3(a) (solid red curve), the gap is evident for the isolated MoS_2 monolayer as shown in Fig. 3(b). When the bilayer of graphene/MoS_2 is formed, the total conductivity, as can be seen in Fig. 3(c), appears to be a linear combination of contributions from each individual mono layers. On the other hand, lithiation causes metallicity in graphene/MoS_2 bilayer, where a large Drude peak appears near the zero frequency Fig. 3(d).

In this letter, bonding between graphene and MoS_2 monolayers has been studied by using DFT-based first-principles theory without and with intercalated Li atoms. Formation of a stable heterostructure between the layers is observed, where the major contribution to binding comes from the vdW interaction. Our calculations show that the addition of the graphene layer pins the Fermi energy near the gap center of MoS_2. Precise identification of the Fermi energy opens up the potential applications for LIB anode material through the manipulation of electronic structure of various constituent element combination with graphene/MoS_2 bilayer. Lithium insertion or intercalation between graphene/MoS_2 bilayer is found to have a binding energy within the physisorption range in our calculations, which demonstrates their potential as superior anode materials. Therefore, our proof-of-principles calculations of adsorption energy, structural stability, electronic structure, and optical properties in graphene/MoS_2 heterostructure provide a basis for future experimental and theoretical study towards designing the next generation anodes for lithium ion batteries.

We thank Jinkyoung Yoo and Enkeleda Dervishi for stimulating discussions. This work was carried out under the auspices of the National Nuclear Security Administration of the U.S. DOE at Los Alamos National Laboratory under Contract No. DE-AC52-06NA25396 and at Sandia National Laboratories under Contract No. DE-AC04-94AL85000. It was supported by the U.S. DOE Office of Basics Energy Sciences (T.A.) and was in part by the Center for Integrated Nanotechnologies—a U.S. DOE BES user facility (N.A.M. & J.-X.Z.).

[1]R. Cuenca and L. Gaines, Center for Transportation Research, Argonne National Laboratory, Argonne, Technical Report No. ANL/ESD-42, 2000.
[2]M. M. Doeff, *Battery Cathodes* (Springer, 2013), pp. 5–49.
[3]G. Wang, X. Shen, J. Yao, and J. Park, Carbon **47**, 2049 (2009), ISSN 0008-6223.
[4]K. Chang and W. Chen, ACS Nano **5**, 4720 (2011).
[5]D. Wang, R. Kou, D. Choi, Z. Yang, Z. Nie, J. Li, L. V. Saraf, D. Hu, J. Zhang, G. L. Graff *et al.*, ACS Nano **4**, 1587 (2010).
[6]X. X. Wang, J. N. Wang, and L. F. Su, J. Power Sources **186**, 194 (2009), ISSN 0378-7753.
[7]H. Wang, L.-F. Cui, Y. Yang, H. Sanchez Casalongue, J. T. Robinson, Y. Liang, Y. Cui, and H. Dai, J. Am. Chem. Soc. **132**, 13978 (2010).
[8]Z.-S. Wu, W. Ren, L. Wen, L. Gao, J. Zhao, Z. Chen, G. Zhou, F. Li, and H.-M. Cheng, ACS Nano **4**, 3187 (2010).
[9]R. Haering, J. Stiles, and K. Brandt, "Lithium molybdenum disulphide battery cathode," U.S. patent 4,224,390 (1980).
[10]Y. Liu, Y. Zhao, L. Jiao, and J. Chen, J. Mater. Chem. A **2**, 13109 (2014).
[11]A. K. Geim and I. V. Grigorieva, Nature **499**, 419 (2013).
[12]K. T. Chan, J. B. Neaton, and M. L. Cohen, Phys. Rev. B **77**, 235430 (2008).
[13]R. H. Miwa and W. L. Scopel, J. Phys.: Condens. Matter **25**, 445301 (2013).
[14]H. Rydberg, M. Dion, N. Jacobson, E. Schröder, P. Hyldgaard, S. I. Simak, D. C. Langreth, and B. I. Lundqvist, Phys. Rev. Lett. **91**, 126402 (2003).
[15]J. Klimeš, D. R. Bowler, and A. Michaelides, J. Phys.: Condens. Matter **22**, 022201 (2010).
[16]Gold Peak Industries Ltd., *Lithium Ion Technical Handbook* (Gold Peak Industries Ltd., 2003).
[17]G. Kresse and J. Furthmüller, Phys. Rev. B **54**, 11169 (1996).
[18]G. Kresse and J. Hafner, Phys. Rev. B **47**, 558 (1993).
[19]G. Kresse and J. Furthmller, Comput. Mater. Sci. **6**, 15 (1996), ISSN 0927-0256.
[20]J. P. Perdew, K. Burke, and M. Ernzerhof, Phys. Rev. Lett. **77**, 3865 (1996).
[21]D. Vanderbilt, Phys. Rev. B **41**, 7892 (1990).
[22]G. Kresse and J. Hafner, J. Phys.: Condens. Matter **6**, 8245 (1994).
[23]J. C. V. Klimeš, D. R. Bowler, and A. Michaelides, Phys. Rev. B **83**, 195131 (2011).
[24]M. Gajdoš, K. Hummer, G. Kresse, J. Furthmüller, and F. Bechstedt, Phys. Rev. B **73**, 045112 (2006).
[25]T. Wehling, A. Black-Schaffer, and A. Balatsky, Adv. Phys. **63**, 1 (2014).
[26]D. Abergel, V. Apalkov, J. Berashevich, K. Ziegler, and T. Chakraborty, Adv. Phys. **59**, 261 (2010).
[27]K. F. Mak, C. Lee, J. Hone, J. Shan, and T. F. Heinz, Phys. Rev. Lett. **105**, 136805 (2010).
[28]H. Shi, H. Pan, Y.-W. Zhang, and B. I. Yakobson, Phys. Rev. B **87**, 155304 (2013).
[29]J. K. Ellis, M. J. Lucero, and G. E. Scuseria, Appl. Phys. Lett. **99**, 261908 (2011).
[30]See supplementary material at http://dx.doi.org/10.1063/1.4927611 for the DOS and corresponding bandstructure in Figs. S1–S4.
[31]C. Ambrosch-Draxl and J. O. Sofo, Comput. Phys. Commun. **175**, 1 (2006), ISSN 0010-4655.

This article is copyrighted as indicated in the article. Reuse of AIP content is subject to the terms at: http://scitation.aip.org/termsconditions. Downloaded to IP: 198.102.153.1 On: Mon, 14 Sep 2015 22:11:18